Rev. Ivoir. Sci. Technol., 43 (2024) 100 - 121
ISSN 1813-3290, http://www.revist.ci

CONOIDAL CRACK WITH ELLIPTIC BASES, WITHIN CUBIC CRYSTALS, UNDER ARBITRARILY APPLIED LOADINGS - I. DISLOCATION, CRACK-TIP STRESS AND CRACK EXTENSION FORCE

P. N. B. ANONGBA

Université F.H.B. de Cocody, U.F.R. Sciences des Structures de la Matière et de Technologie, 22 BP 582 Abidjan 22, Côte d'Ivoire

(reçu le 28 Avril 2024; accepté le 10 Juin 2024)

* Correspondance, e-mail : *anongba@gmail.com*

ABSTRACT

Conoidal cracks with elliptical bases within cubic crystals are investigated. Under general loading (tension and shears), the crack is represented by a continuous distribution of three dislocation families m (m= 1, 2 and 3). Expressions for the elastic fields (displacement $\boldsymbol{u}^{(m)}$and stress $(\sigma)^{(m)}$) of the crack dislocations with elliptic forms are provided. Spatial dependences of the dislocation distribution D_m at equilibrium, about the crack-tip, are obtained with associated relative displacements ϕ_m of the faces of the crack. These lead to analytical expressions for crack-tip stresses and crack extension force G per unit length of the crack front. By using the word "twin" instead of "crack", it is stressed that this study applies entirely when abundant twinning is the mode of deformation adopted by the loaded cubic material. For definiteness, is exemplified the observed mechanical twinning in temperature regime 2 (773 to 1173K) in [112] copper single crystals deformed at constant strain rates (stage V).

Keywords : *fracture mechanics, linear elasticity, dislocations, crack extension force, high temperature mechanical twinning.*

RÉSUMÉ

Fissure conoïdale à base elliptique dans un cristal cubique sous sollicitations extérieures arbitraires – I. Dislocation, contrainte en tête de fissure et force d'extension de fissure

Des fissures conoïdales à bases elliptiques à l'intérieur de cristaux cubiques sont étudiées. Sous chargement général (traction et cisaillement), la fissure est représentée par une distribution continue de trois familles de dislocations m (m = 1, 2 et 3). Des expressions pour les champs élastiques (déplacement $\boldsymbol{u}^{(m)}$ et contrainte $(\sigma)^{(m)}$) des dislocations de fissures de forme elliptique sont fournies. Les dépendances spatiales des distributions de dislocation D_m à l'équilibre, au niveau du fond de fissure, sont obtenues avec les déplacements relatifs ϕ_m associés des faces de la fissure. Celles-ci conduisent à des expressions analytiques pour les contraintes aux extrémités de fissure et la force d'extension de fissure G par unité de longueur du front de fissure. En utilisant le mot ″macle″ au lieu de ″fissure″, on souligne que cette étude s'applique entièrement lorsqu'un maclage abondant est le mode de déformation adopté par le matériau cubique chargé. Pour plus de précision, est illustré le maclage mécanique observé dans le régime de température 2 (773 à 1173 K) dans des monocristaux de cuivre d'axe [112] déformés à des vitesses de déformation constantes (stade V).

Mots-clés : *mécanique de la rupture, élasticité linéaire, dislocation, force d'extension de fissure, maclage mécanique à haute temperature.*

I - INTRODUCTION

Recent works [1 - 3] have investigated rough conoidal cracks with average circular bases under general loading in isotropic materials. The present study focusses on smooth conoidal cracks (vertex O) with elliptical bases in cubic crystals; the elliptic form of the bases is expected in anisotropic media. The model is illustrated in ***Figure 1***.

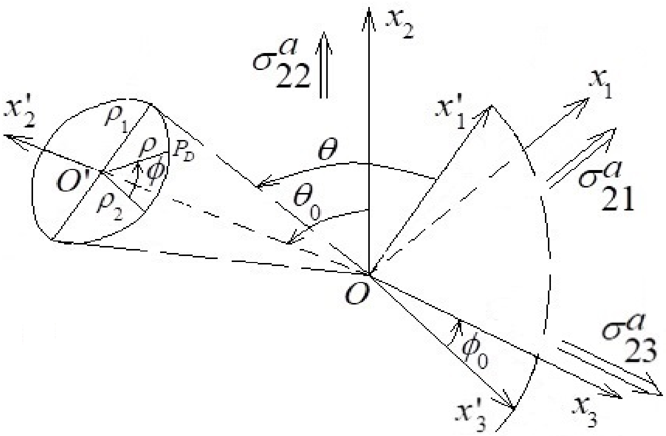

Figure 1 : *Elliptical base (elevation* $x'_2 = OO' \equiv h$*) of the conoidal crack with semiaxes* ρ_1 *and* ρ_2 *along* x'_1 *and* x'_3*. The running point* P_D (1) *along the base and angular parameters* θ_0 *and* ϕ_0 *that connect* $\mathbf{x}_j$ *and* $\vec{x}'_j$ *are illustrated. Angle* θ *is introduced by the relation* $\tan\theta = OO'/\rho_1$. *The medium suffers uniformly applied tension* σ^a_{22} *in the vertical* x_2 *- direction and shears* σ^a_{21} *and* σ^a_{23} *(parallel to the horizontal* x_1x_3*- plane) in the* x_1 *and* x_3 *directions*

The medium is infinitely extended in the Ox_j- directions (laboratory Cartesian reference frame). The stresses are uniform, applied at infinity, with tension σ_{22}^{a} and shears σ_{21}^{a} and σ_{23}^{a} in the x_2, x_1 and x_3 directions, respectively. Induced normal Poisson's stresses $-\nu_A(j)\sigma_{22}^{a}$ along x_1 (j = 1) and x_3 (j = 3) are considered. The crack nuclei are arbitrarily oriented with attached Cartesian ($O; x_j^{'}$); $O x_2^{'}$ is a symmetrical axis. In $x_1^{'}x_3^{'}-$planes, the bases are elliptical with semiaxes ρ_1 and ρ_2 along $x_1^{'}$ and $x_3^{'}$ such that $a_r = \rho_1 / \rho_2$ = constant about any elevation $x_2^{'} = OO' \equiv h$ along $O x_2^{'}$. The running position P_D ($x_1^{'}, x_2^{'}, x_3^{'}$) at the elevation h along the base is written with respect to ($O; x_j^{'}$) as

$$\overrightarrow{OP}_D = \begin{pmatrix} x_1^{'} = \rho \sin\phi \\ x_2^{'} = h = \rho_1 \tan\theta \\ x_3^{'} = \rho \cos\phi \end{pmatrix}; \ -\pi \le \phi \le \pi, \quad 0 \le \theta < \pi/2;$$

$$\rho^2 = \rho_1^2 / (\sin^2\phi + a_r^2 \cos^2\phi). \tag{1}$$

The angle ϕ is between $O' x_3^{'}$ and $O'P_D$ as shown in ***Figure 1***. Angle θ is measured in $O x_1^{'} x_2^{'}$ between $\boldsymbol{P_D}$ ($\phi = \pi/2$) ***O'*** and $\boldsymbol{P_D}$ ($\phi = \pi/2$) ***O*** where P_D ($\phi = \pi/2$) has elevation $x_2^{'} = h$ from $O x_1^{'} x_3^{'}$; its alternate interior angle is shown in ***Figure 1***. Additional angular parameters θ_0 and ϕ_0 (Euler's angles) are introduced that connect $\vec{x}_j$ to $\vec{x}_j^{'}$:

- θ_0 (the angle of nutation) defined by unit vectors $\boldsymbol{x}_2$ and $\vec{x}_2^{'}$, the growing sense corresponds to the rotation around $\boldsymbol{x}_3$ (the corkscrew rule applies),
- ϕ_0 (the proper rotation angle) defined by unit vectors $\boldsymbol{x}_3$ and $\vec{x}_3^{'}$, the growing sense corresponds to the rotation around $\vec{x}_2^{'}$.

The crack is represented by a continuous distribution of three dislocation families with Burgers vectors $\boldsymbol{b}_j = b\,\vec{x}_j^{'}$, directed along positive $\vec{x}_j^{'}$, and running point P_D (1) at the height $x_2^{'} = OO' \equiv h$ along $O x_2^{'}$ (see ***Figure 1***). Distribution functions D_j of the crack dislocations j are defined such that D_j (ρ_1) $d\rho_1$ represents the number of dislocations j in a small interval $d\rho_1$ located at the position $x_1^{'} = \rho_1$ on the $O \vec{x}_1^{'}$- axis ($- a_1 \le x_1^{'} = \rho_1 \le a_1$); D_j (ρ_1)= D_j (- ρ_1) by symmetry, this restricts ourselves to positive $x_1^{'}$ values. The elastic fields in the fractured medium read as a superposition of those due to elliptical crack dislocations. In *Section* 2 (Methodology), the procedures for determining the elastic fields of the dislocations and crack analysis are explained. In *Section* 3, are given the elastic fields (stress and displacement) of the elliptical dislocations j, distribution functions D_j of the crack dislocations and corresponding relative displacement ϕ_j of the faces of the crack, crack-tip stress, and crack extension force G per unit length of the crack front. *Section* 4 and 5 are devoted to discussion and conclusion, respectively.

II - METHODOLOGY

II-1. Elastic fields of elliptical crack dislocations in cubic crystals

The three types j (j=1, 2 and 3) of crack dislocation considered have Burgers vectors $\vec{b}_1 = (b,0,0)$, $\vec{b}_2 = (0,b,0)$ and $\vec{b}_3 = (0,0,b)$ along $x_j^{'}$; they spread in the $O'x_1^{'}x_3^{'}$-plane in the form (1). We shall make use of the displacement $\bar{u}_m(\vec{x}^{'})$, m=1, 2 and 3, and $\bar{\sigma}_{pq}(\vec{x}^{'})$ due to a plastic distortion $\beta_{ij}^{*}(\vec{x}^{'})$ given as a periodic function of coordinates $\vec{x}^{'} = (x_1^{'}, x_2^{'}, x_3^{'})$

$$\beta_{ij}^{*} = \bar{\beta}_{ij}^{*}(\vec{k}^{'})e^{i\vec{k}'.\vec{x}'} \tag{2}$$

where $\vec{k}^{'} = (k_1^{'}, k_2^{'}, k_3^{'})$ with $k_j^{'}$ arbitrary constants. Mura [4] has shown the associated elastic fields to be

$$\begin{aligned}
&\bar{u}_m(\vec{x}^{'}) = -ik_l^{'}C_{klij}L_{mk}\bar{\beta}_{ji}^{*}e^{i\vec{k}'.\vec{x}'} ,\\
&\bar{\sigma}_{pq}(\vec{x}^{'}) = C_{pqmn}\left(k_n^{'}k_l^{'}C_{klij}L_{mk}\bar{\beta}_{ji}^{*} - \bar{\beta}_{nm}^{*}\right)e^{i\vec{k}'.\vec{x}'} ,\\
&L_{mk} = \frac{\in_{kst}\in_{mnr}\left(C_{sjnl}k_l^{'}k_j^{'}\right)\left(C_{tjrl}k_l^{'}k_j^{'}\right)}{2\in_{pqr}\left(C_{pj1l}k_l^{'}k_j^{'}\right)\left(C_{qj2l}k_l^{'}k_j^{'}\right)\left(C_{rj3l}k_l^{'}k_j^{'}\right)} .
\end{aligned} \tag{3}$$

Here forms like $\in_{njh}$ correspond to the permutation unit tensor (all zero except the permutations of $\in_{123}$ with respect to the indices, using 1 for even and -1 for odd permutations). We stress that the so-called summation convention is used throughout this work: if a subscript is repeated, summation from 1 to 3 is implied.

$$C_{ijkl} = \lambda \delta_{ij} \delta_{kl} + \mu \delta_{ik} \delta_{jl} + \mu \delta_{il} \delta_{jk} + \mu' \delta_{ijkl} \tag{4}$$

where all $\delta_{ijkl} = 0$ except $\delta_{1111} = \delta_{2222} = \delta_{3333} = 1$ and

$$\lambda = C_{12} \ , \quad \mu = C_{44} \ , \quad \mu' = C_{11} - C_{12} - 2C_{44} \ . \tag{5}$$

δ_{ij} in (4) is the Kronecker delta; the C_{ij} in (5) are the Voigt constants. The constants C_{ijkl} are symmetrical as follows,

$$C_{ijkl} = C_{ijlk} = C_{klij} = C_{jikl} \ . \tag{6}$$

The plastic distortions $\beta_{ij}^{*(l)}$, associated to the elliptical crack dislocations l (l= 1, 2 and 3) at the height h= *OO'* in the distribution (***Figure* 1**), are expressed successively at $\vec{x}' = (x_1', x_2', x_3')$.

$$\begin{aligned} \beta_{21}^{*(1)} &= b\delta(y_2')\left(H\left[x_1' + \sqrt{\rho_1^2 - a_r^2 x_3'^2} \right] - H\left[x_1' - \sqrt{\rho_1^2 - a_r^2 x_3'^2} \right] \right), \quad |x_3'| \le \rho_2 \\ &= \frac{b\rho_1}{(2\pi)^2} \int_{-\infty}^{\infty}\int_{-\infty}^{\infty}\int_{-\infty}^{\infty} \frac{J_1[\eta_2]}{\sqrt{k_3'^2 + a_r^2 k_1'^2}} e^{i\vec{k}'.\vec{x}_h'} d\vec{k}' \ . \end{aligned} \tag{7}$$

$\eta_2 = (\rho_1 / a_r)\sqrt{k_3'^2 + a_r^2 k_1'^2}$, $J_1[\eta_2]$ is the Bessel function of the first kind; $\vec{k}' = (k_1', k_2', k_3')$, $\vec{x}_h' = (x_1', x_2' - h \equiv y_2', x_3')$, $d\vec{k}' = dk_1' dk_2' dk_3'$ and δ and H are the Dirac delta and Heaviside step functions, respectively. $\beta_{21}^{*(1)} = 0$ for $|x_3'| \ge \rho_2$. The other components of the plastic distortion are zero. $\beta_{21}^{*(1)}$ (7) in its Fourier form is a superposition of expressions of the form (2). Therefore, associated displacement and stress are similar superpositions of (3), hence,

$$\begin{aligned} u_m^{(1)}(\vec{x}') &= -\int_{-\infty}^{\infty}\int_{-\infty}^{\infty}\int_{-\infty}^{\infty} ik_l' C_{kl12} L_{mk} \overline{\beta}_{21}^{*(1)} e^{i\vec{k}'.\vec{x}_h'} d\vec{k}' \ , \\ \sigma_{pq}^{(1)}(\vec{x}') &= \int_{-\infty}^{\infty}\int_{-\infty}^{\infty}\int_{-\infty}^{\infty} C_{pqmn}\left(k_n' k_l' C_{kl12} L_{mk} \overline{\beta}_{21}^{*(1)} - \overline{\beta}_{nm}^{*(1)} \right) e^{i\vec{k}'.\vec{x}_h'} d\vec{k}' , \\ \overline{\beta}_{21}^{*(1)} &= \frac{b\rho_1}{(2\pi)^2} \frac{J_1[\eta_2]}{\sqrt{k_3'^2 + a_r^2 k_1'^2}} \end{aligned} \tag{8}$$

$\overline{\beta}_{nm}^{*(1)}$ are zero except $\overline{\beta}_{21}^{*(1)}$. Performing the necessary integrations in (8) provide the elastic fields of the elliptical dislocations j=1 at the elevation h in the conoidal crack dislocation distribution ***(Figure 1)*** in Cartesian coordinates $x_j^{'}$. We now consider the dislocation j= 2 with form (1) and Burgers vector $\vec{b}_2 = (0, b, 0)$ along $x_2^{'}$. There are only two non-zero components $\beta_{12}^{*(2)}$ and $\beta_{32}^{*(2)}$ of the plastic distortion.

$$\beta_{12}^{*(2)} = bH(y_2^{'})\left(\delta\left[x_1^{'} + \sqrt{\rho_1^2 - a_r^2 x_3^{'2}}\right] - \delta\left[x_1^{'} - \sqrt{\rho_1^2 - a_r^2 x_3^{'2}}\right]\right)$$
$$= \int_{-\infty}^{\infty}\int_{-\infty}^{\infty}\int_{-\infty}^{\infty} \frac{k_1^{'}}{k_2^{'}} \overline{\beta}_{21}^{*(1)} e^{i\vec{k}'.\vec{x}_h^{'}} d\vec{k}^{'} \equiv \int_{-\infty}^{\infty}\int_{-\infty}^{\infty}\int_{-\infty}^{\infty} \overline{\beta}_{12}^{*(2)} e^{i\vec{k}'.\vec{x}_h^{'}} d\vec{k}^{'};$$
$$\beta_{32}^{*(2)} = bH(y_2^{'})\left(\delta\left[x_3^{'} + a_r^{-1}\sqrt{\rho_1^2 - x_1^{'2}}\right] - \delta\left[x_3^{'} - a_r^{-1}\sqrt{\rho_1^2 - x_1^{'2}}\right]\right)$$
$$= \int_{-\infty}^{\infty}\int_{-\infty}^{\infty}\int_{-\infty}^{\infty} \frac{k_3^{'}}{k_2^{'}} \overline{\beta}_{21}^{*(1)} e^{i\vec{k}'.\vec{x}_h^{'}} d\vec{k}^{'} \equiv \int_{-\infty}^{\infty}\int_{-\infty}^{\infty}\int_{-\infty}^{\infty} \overline{\beta}_{32}^{*(2)} e^{i\vec{k}'.\vec{x}_h^{'}} d\vec{k}^{'}. \tag{9}$$

Making use of (3) , we obtain

$$u_m^{(2)} = -\int_{-\infty}^{\infty}\int_{-\infty}^{\infty}\int_{-\infty}^{\infty} ik_l^{'} L_{mk}\left(C_{kl21}\overline{\beta}_{12}^{*(2)} + C_{kl23}\overline{\beta}_{32}^{*(2)}\right) e^{i\vec{k}'.\vec{x}_h^{'}} d\vec{k}^{'},$$
$$\sigma_{pq}^{(2)} = \int_{-\infty}^{\infty}\int_{-\infty}^{\infty}\int_{-\infty}^{\infty} C_{pqmn}\left(k_n^{'}k_l^{'}L_{mk}\left[C_{kl21}\overline{\beta}_{12}^{*(2)} + C_{kl23}\overline{\beta}_{32}^{*(2)}\right] - \overline{\beta}_{nm}^{*(2)}\right) e^{i\vec{k}'.\vec{x}_h^{'}} d\vec{k}^{'}.$$
(10)

We consider the dislocation j= 3 with form (1) and Burgers vector $\vec{b}_3 = (0, 0, b)$ along $x_3^{'}$. For the plastic distortion, we have

$$\beta_{23}^{*(3)} = b\delta(y_2^{'})H\left(\left[x_1^{'} + \sqrt{\rho_1^2 - a_r^2 x_3^{'2}}\right]\left[\sqrt{\rho_1^2 - a_r^2 x_3^{'2}} - x_1^{'}\right]\right), \quad \left|x_3^{'}\right| \le \rho_2$$
$$= \int_{-\infty}^{\infty}\int_{-\infty}^{\infty}\int_{-\infty}^{\infty} \overline{\beta}_{21}^{*(1)} e^{i\vec{k}'.\vec{x}_h^{'}} d\vec{k}^{'}, \quad \overline{\beta}_{23}^{*(3)} = \overline{\beta}_{21}^{*(1)}; \tag{11}$$

$\beta_{23}^{*(3)} = 0$ for $\left|x_3^{'}\right| \ge \rho_2$ and the other components of the plastic distortion are zero. (11) and (7) are identical although their Cartesian form is written differently. Making use of (3), we obtain,

$$u_m^{(3)} = -\int_{-\infty}^{\infty}\int_{-\infty}^{\infty}\int_{-\infty}^{\infty} ik_l^{'} C_{kl32} L_{mk} \overline{\beta}_{23}^{*(3)} e^{i\vec{k}'.\vec{x}_h^{'}} d\vec{k}',$$

$$\sigma_{pq}^{(3)} = \int_{-\infty}^{\infty}\int_{-\infty}^{\infty}\int_{-\infty}^{\infty} C_{pqmn} \left(k_n^{'} k_l^{'} C_{kl32} L_{mk} \overline{\beta}_{23}^{*(3)} - \overline{\beta}_{nm}^{*(3)} \right) e^{i\vec{k}'.\vec{x}_h^{'}} d\vec{k}'. \quad (12)$$

At this stage, we can write down the various elastic fields displacements $\vec{u}^{(j)}$ and $(\sigma)^{(j)}$ associated with the three types j of crack dislocation with form (1). Our calculation results are displayed in Section 3.

II-2. Crack analysis

We shall apply the traction-free condition at any position on the crack boundary. This gives:

$$\begin{cases} \overline{\sigma}_{12} - \overline{\sigma}_{11} \partial x_2^{'} / \partial x_1^{'} - \overline{\sigma}_{13} \partial x_2^{'} / \partial x_3^{'} = 0 \\ \overline{\sigma}_{22} - \overline{\sigma}_{21} \partial x_2^{'} / \partial x_1^{'} - \overline{\sigma}_{23} \partial x_2^{'} / \partial x_3^{'} = 0 \\ \overline{\sigma}_{32} - \overline{\sigma}_{31} \partial x_2^{'} / \partial x_1^{'} - \overline{\sigma}_{33} \partial x_2^{'} / \partial x_3^{'} = 0 \end{cases} \quad (13)$$

$\overline{\sigma}_{ij}$ stands for the total stress at any point $P(x_1^{'}, x_2^{'}, x_3^{'})$ in the medium and is linked to the crack dislocation distribution D_j. (13) concerns the positions on the crack faces only. $\overline{\sigma}_{ij}$ is written as (relatively to $x_j^{'}$)

$$\overline{\sigma}_{ij} = \sigma_{ij}^{'A} + \sigma_{ij}^{(C)(1)} + \sigma_{ij}^{(C)(2)} + \sigma_{ij}^{(C)(3)} \quad (14)$$

$(\sigma')^A$ is the externally applied stress including normal induced stresses from Poisson effect; relatively to $x_j^{'}$, its components are given in *Appendix A*.

$$\sigma_{ij}^{(C)(m)}(\vec{x}') = \int_0^{a_1} \sigma_{ij}^{(m)}(\vec{x}'; \rho_1) D_m(\rho_1) d\rho_1 \qquad (m = 1, 2 \text{ and } 3) \quad (15)$$

Here we assume that the crack extends from 0 to a_1 along positive values on the $O x_1^{'}$- axis. $\sigma_{ij}^{(m)}$ is the stress field at $\vec{x}'$ due to a conoidal crack dislocation m with position $x_1^{'} = \rho_1$ along $O x_1^{'}$ in the dislocation distribution. (13) give three integral equations the resolution of which yields the D_m. The relative displacements ϕ_m of the faces of the crack in the $x_m^{'}$- direction at the position

P_D (1) in the distribution are obtained by integration from the relation $d\phi_m = -bD_m(\rho_1)d\rho_1$:

$$\phi_m = \int_{\rho_1}^{a_1} bD_m(\rho')d\rho', \qquad 0 \le \rho_1 \le a_1 \text{ and } 0 \le \phi \le \pi \,. \tag{16}$$

From (14) to (15), one can obtain the crack-tip stresses. The crack extension force G per unit length of the crack front is defined in previous works (see [1-3, 5], for example). The presentations in [1, 3] best correspond to the present study. The front of the crack ***(Figure 1)*** with shape (say P_D, (1) with $\rho_1 = a_1$) is assumed to advance steadily from $\rho_1 = a_1$ (shorter crack) to $\rho_1 = a_1 + \delta a_1$ (lengthened crack). At an arbitrary position P_D (1) with $a_1 \le \rho_1 \le a_1 + \delta a_1$, is attached a surface element $\overrightarrow{ds}$ that reads

$$\overrightarrow{ds} = \begin{pmatrix} ds_1 \\ ds_2 \\ ds_3 \end{pmatrix} = -d\rho_1 d\phi \frac{\rho_1 \tan\theta}{a_r^3 g_1^{3/2}(\phi)} \begin{pmatrix} \sin\phi \\ -a_r^2 g_1(\phi) \\ a_r^2 \cos\phi \end{pmatrix}_{x_j'} , \tag{17}$$

$$g_1(\phi) = a_r^{-2}\sin^2\phi + \cos^2\phi \,.$$

The component of the force acting on ds in the x_i' – direction is $\bar{\sigma}_{ij} ds_j$ (the summation convention on repeated subscripts applies) where $\bar{\sigma}_{ij}$ are stresses ahead of the shorter or behind the lengthened crack; thus the energy change associated with ds is $\bar{\sigma}_{ij} ds_j \Delta u^{(i)}/2$ (here a summation is also considered over $i = 1$, 2 and 3) where $\Delta u^{(i)}$ is the difference in displacement across the lengthened crack, just behind its tip, in the x_i' – direction. When the crack advances from $\rho_1 = a_1$ to $\rho_1 = a_1 + \delta a_1$, the energy decrease associated with a surface element

$$\Delta s = \int_{\rho_1 = a_1}^{a_1 + \delta a_1} ds(P_D) \cong \delta a_1 d\phi \overline{\Delta s}$$

$$\overline{\Delta s} = a_1 \tan\theta a_r^{-3} g_1^{-3/2}(\phi) \sqrt{\sin^2\phi\cos^2\phi(1 - a_r^2)^2 + 2a_r^4 g_1^2(\phi)} \tag{18}$$

(δa_1 being small and, when used below, will be let to go to zero) is given as

$$-\delta E = \frac{1}{2}\int_{a_1}^{a_1+\delta a_1} \sum_i \sum_j \bar{\sigma}_{ij} ds_j \Delta u^{(i)} , \tag{19}$$

the integration being performed with respect to ρ_1; we stress that Δs is the sum of the surface elements ds taken at the various points P_D (1) as ρ_1 only changes from a_1 to $a_1 + \delta a_1$. The crack extension force G per unit length of the crack front at $P_0 = P_D$ (with $\rho_1 = a_1$, ϕ given) is defined as

$$G(P_0) = \lim_{\delta a_1 \to 0} -\delta E / \Delta s . \tag{20}$$

III - RESULTS

Physical quantities concerned here are the spatial dependence of the crack dislocation distributions D_m about the crack front, the crack-tip stresses $\bar{\sigma}_{ij}$ and the crack extension force G per unit length of the crack front. These require using the stress fields $\sigma_{ij}^{(m)}$ of those dislocations located at the very tip of the crack front. Hence, are displayed first below stresses $\sigma_{ij}^{(m)}$ to linear terms with respect to ($x_2^{'} - h$).

III-1. Stresses $\sigma_{ij}^{(m)}(\vec{x}';\rho_1)$ to linear terms with respect to ($x_2^{'} - h$)

The dislocations m have elevation h in the distribution and semiaxes ρ_1 and ρ_2 ($a_r = \rho_1 / \rho_2$) along $O x_1^{'}$ and $O x_3^{'}$, respectively, under the condition $x_2^{'} < h$ from the crack-tip stress calculations below. Associated stresses are displayed in *Appendix B.*

III-2. Conoidal crack dislocation distributions D_m

The traction-free conditions (13) are written for positions $P_C = (x_1^{'},\ x_2^{'} = x_1^{'} \tan\theta ,\ x_3^{'} = 0)$ that correspond to $\boldsymbol{OP_D}$ ($\phi = \pi/2$) (1); the crack front is assumed located at $x_1^{'} = a_1$ on the $x_1^{'}$-axis. This reduces to

$$\begin{cases} \bar{\sigma}_{12} - \bar{\sigma}_{11} \tan\theta = 0 \\ \bar{\sigma}_{22} - \bar{\sigma}_{21} \tan\theta = 0 . \\ \bar{\sigma}_{32} - \bar{\sigma}_{31} \tan\theta = 0 \end{cases} \tag{21}$$

Only the spatial dependence of D_m about the crack front is required in the crack analysis. Hence, P_C will be moved closer to the crack-tip *i.e.* $a_1 - \delta a_1 < x_1^{'} \leq a_1$ $(0 < \delta a_1 \leq a_1)$. $\sigma_{ij}^{(C)(m)}$ when used in (21) is identified to

$$\sigma_{ij}^{(C)(m)}(P_C) = \int_{x_1^{'}}^{a_1} \sigma_{ij}^{(m)}(P_C;\overline{x}_1) D_m(\overline{x}_1) d\overline{x}_1 \tag{22}$$

where $\sigma_{ij}^{(m)}$ is the stress at P_C due to a conoidal crack dislocation m with position $x_1^{'} = \overline{x}_1$ (height $x_2^{'} = \overline{h} \equiv \overline{x}_1 \tan\theta$) along $x_1^{'}$; hence, $a_1 - \delta a_1 < x_1^{'} < \overline{x}_1 < a_1$. Essentially, dislocation loops with $\overline{x}_1 < x_1^{'}$ contribute nothing. Under such conditions, (21) can be managed to provide three singular integral equations with the simple Cauchy type

$$\begin{aligned}
&Term(1) + \frac{b\pi}{(2\pi)^2 C_{11} a_r} \int_{1-\delta a_1/a_1}^{1} d\overline{z}_1 \frac{D_1(\overline{z}_1)}{1-\overline{z}_1} = 0,\\
&Term(2) + \frac{b\pi}{(2\pi)^2 C_{11} 3a_r} \int_{1-\delta a_1/a_1}^{1} d\overline{z}_1 \frac{D_2(\overline{z}_1)}{1-\overline{z}_1} = 0,\\
&\sigma'^{A}_{32} - \tan\theta\sigma'^{A}_{31} - \frac{bC_{44}(C_{11}+4C_{12})}{6\pi C_{11} a_r} \int_{1-\delta a_1/a_1}^{1} d\overline{z}_1 \frac{D_3(\overline{z}_1)}{1-\overline{z}_1} = 0;
\end{aligned} \tag{23}$$

$$\begin{aligned}
&Term(1) = \frac{K_{13}^{(2)}\left[\sigma'^{A}_{22} - \tan\theta\sigma'^{A}_{21}\right] + K_{23}^{(2)}\left[\sigma'^{A}_{12} - \tan\theta\sigma'^{A}_{11}\right]}{K_{13}^{(2)}K_{22}^{(1)} + K_{23}^{(2)}K_{12}^{(1)}},\\
&Term(2) = \frac{K_{12}^{(1)}\left[\sigma'^{A}_{22} - \tan\theta\sigma'^{A}_{21}\right] - K_{22}^{(1)}\left[\sigma'^{A}_{12} - \tan\theta\sigma'^{A}_{11}\right]}{K_{13}^{(2)}K_{22}^{(1)} + K_{23}^{(2)}K_{12}^{(1)}};
\end{aligned} \tag{24}$$

$$\begin{aligned}
&K_{22}^{(1)} = \tan\theta\left(2C_{11}(C_{44}+C_{12}) - (C_{11}^2 + C_{12}C_{44} + 2C_{44}^2)\right),\\
&K_{23}^{(2)} = 4\left[C_{11}^2 + C_{12}C_{44} + C_{11}(C_{44}+C_{12})\right] + 9\tan^2\theta C_{44}^2,\\
&K_{12}^{(1)} = 2C_{44}^2 - \tan^2\theta\left(2(C_{12}C_{44} + C_{11}^2) - C_{11}(C_{12}+C_{44})\right),\\
&K_{13}^{(2)} = \tan\theta\left(9C_{44}^2 + 4\left[C_{11}(C_{44}+C_{12}) + C_{12}C_{44} + C_{11}^2\right]\right);
\end{aligned} \tag{25}$$

$(\sigma')^A$ is given in *Appendix A*. (23) are inverted in a similar way as in [3] to give

$$D_m \cong \alpha_0 \alpha_m \frac{1}{\sqrt{1-z_1}}, \qquad m=1,\ 2 \text{ and } 3, \tag{26}$$

$z_1 = x_1^{'} / a_1$, $(1 - z_1)$ positive infinitesimal value and α_0 a dimensionless constant [3];

$$\alpha_1 = \frac{4a_r C_{11}}{b} Term(1) ,$$

$$\alpha_2 = \frac{12a_r C_{11}}{b} Term(2) ,$$

$$\alpha_3 = -\frac{6a_r C_{11}}{bC_{44}(C_{11}+4C_{12})}\left[\sigma'^{A}_{32} - \tan\theta\sigma'^{A}_{31}\right] \equiv -\frac{6a_r C_{11}}{b} Term(3) . \qquad (27)$$

(26) is the value of dislocation m distribution closer to the crack tip. The associated relative displacement ϕ_m of the faces of the crack is,

$$\phi_m \cong 2b\alpha_0\alpha_m a_1\sqrt{1-z_1} \ . \qquad (28)$$

III-3. Crack-tip stresses

We assume the crack front to move from the elevation $h(a_1) = a_1 \tan\theta$ to $h(a_1+\delta a_1) = (a_1+\delta a_1) \tan\theta$ along $x_2^{'}$ (use ***Figure 1*** for illustration) and consider a position $P(x_1^{'}, x_2^{'}, x_3^{'})$ on the newly created crack boundary with $x_2^{'} = \bar{x}_1^{'} \tan\theta$, $a_1 \leq \bar{x}_1^{'} < a_1+\delta a_1$. P is given by $P_D(1)$ with $\rho_1 = \bar{x}_1^{'}$. The stress at P is identified to,

$$\bar{\sigma}_{ij}(P) \equiv \sum_{m=1}^{3} \int_{\bar{x}_1^{'}}^{a_1+\delta a_1} \sigma_{ij}^{(m)}(P;\bar{x}_1) D_m(\bar{x}_1) d\bar{x}_1 \equiv \sum_{m=1}^{3} \bar{\sigma}_{ij}^{(m)} \qquad (29)$$

$\sigma_{ij}^{(m)}$ are given in *Section* 3.1. For $D_m(\bar{x}_1)$ we use (26) with $z_1 = \bar{x}_1 / (a_1+\delta a_1)$. Two types of integration with respect to $\bar{x}_1$ are required in the calculation of $\bar{\sigma}_{ij}(P)$. These are:

$$I_t^{(m)}(a) \equiv \int_{\bar{x}_1^{'}}^{a_1+\delta a_1} \bar{x}_1 \left(x_2^{'} - h\right) \mathrm{Re}(I_2) D_m(\bar{x}_1) d\bar{x}_1$$

$$= \frac{\alpha_0\alpha_m 4\tan\theta a_r^3 \sqrt{a_1}\cos(\psi-\phi)(a_1+\delta a_1 - \bar{x}_1^{'})^{3/2}}{\sqrt{g_1(\phi) g_2^2(\psi)}\left(1+\sqrt{\tilde{\omega}}\right)^2 \sqrt{1-\tilde{\omega}}\left(a_1+\delta a_1 - \bar{x}_1^{'}\sqrt{\tilde{\omega}}\right)^2} ,$$

$$I_t^{(m)}(b) \equiv \int_{\bar{x}_1'}^{a_1+\delta a_1} \bar{x}_1 \operatorname{Re}(Q_1) D_m(\bar{x}_1) d\bar{x}_1$$

$$= \frac{\alpha_0 \alpha_m 2a_r^2 \sqrt{a_1}(a_1 + \delta a_1 - \bar{x}_1')^{1/2}}{g_2(\psi)\left(1+\sqrt{\tilde{\omega}}\right)\sqrt{1-\tilde{\omega}}\left(a_1 + \delta a_1 - \bar{x}_1'\sqrt{\tilde{\omega}}\right)} \; ; \tag{30}$$

$$\tilde{\omega} = \frac{\cos^2(\psi - \phi)}{g_1(\phi) g_2(\psi)} \; ; \tag{31}$$

to be introduced in $\bar{\sigma}_{ij}^{(m)}$ to list $\bar{\sigma}_{ij}$ (P) in (29).

III-4. Crack extension force

The procedure for calculating G (20), the crack extension force per unit length of the crack front at P_0, is outlined in *Section* 2. For $\Delta u^{(i)}$ in (19), we use ϕ_i (28) with $z_1 = \bar{x}_1 / (a_1 + \delta a_1)$. $G(P_0)$ is written in the form:

$$G(P_0) = \sum_{n,m,i,j} G_{ij}^{(n)}(m), \quad n, m, i, j = 1, 2 \text{ and } 3. \tag{32}$$

n refer to the relative displacement ϕ_n of the faces of the crack in the $x_n' -$ direction; m correspond to crack dislocation families; ij point out to the stress component $\bar{\sigma}_{ij}$.

$$G_{11}^{(1)}(1) = -\frac{2^7 a_1 \alpha_0^2 a_r^5 C_{11} \tan\theta \sin\phi Term(1)^2}{3\pi g_1^{1/2}(\phi)\Delta^*} \int_{-\pi/2}^{\pi/2} d\psi \frac{\sin\psi \cos(\psi-\phi)}{g_2^{5/2}(\psi)\tilde{\omega}\sqrt{1-\tilde{\omega}}\left(1+\sqrt{\tilde{\omega}}\right)^2}$$
$$\times\left(2\left(C_{12}C_{44} + C_{11}^2\right)\overline{SC}^{1/6} - \frac{F_{11}^{(1)}(a)}{\sqrt{\overline{SC}}} + \frac{4C_{12}C_{11}\cos^2\psi}{\overline{SC}^{1/6}}\right),$$

$$G_{11}^{(1)}(2) = -\frac{4^3 a_1 \alpha_0^2 a_r^4 C_{11} \sin\phi Term(1) Term(2)}{\pi\Delta^*} \int_{-\pi/2}^{\pi/2} \frac{d\psi}{g_2^{3/2}(\psi)\sqrt{\tilde{\omega}}\sqrt{1-\tilde{\omega}}\left(1+\sqrt{\tilde{\omega}}\right)}$$

$$\times\left(\frac{\sin^2\psi F_{11}^{(2)}(a)+C_{12}\cos^2\psi F_{11}^{(2)}(b)}{\overline{SC}^{5/6}}+\frac{F_{11}^{(2)}(c)}{\overline{SC}^{1/6}}-\frac{C_{12}(C_{11}+C_{12})\sin^2\psi\cos^2\psi}{\sqrt{\overline{SC}}}\right),$$

$$G_{11}^{(1)}(3)=0;$$

$$G_{12}^{(1)}(1)=\frac{2^5a_1\alpha_0^2a_r^6C_{44}C_{11}g_1(\phi)Term(1)^2}{3\pi\Delta^*}\int_{-\pi/2}^{\pi/2}\frac{d\psi}{g_2^{3/2}(\psi)\sqrt{\tilde{\varpi}}\sqrt{1-\tilde{\varpi}}\left(1+\sqrt{\tilde{\varpi}}\right)}$$

$$\times\left(\frac{F_{12}^{(1)}(a)}{\overline{SC}^{5/6}}+\frac{F_{12}^{(1)}(c)}{\overline{SC}^{1/6}}+\frac{F_{12}^{(1)}(b)}{\sqrt{\overline{SC}}}\right),$$

$$G_{12}^{(1)}(2)=-\frac{2^7a_1\alpha_0^2a_r^7C_{44}C_{11}\sqrt{g_1}\tan\theta Term(1)Term(2)}{\pi\Delta^*}$$

$$\times\int_{-\pi/2}^{\pi/2}d\psi\frac{\sin\psi\cos(\psi-\phi)}{g_2^{5/2}(\psi)\tilde{\varpi}\sqrt{1-\tilde{\varpi}}\left(1+\sqrt{\tilde{\varpi}}\right)^2}\left(\frac{F_{12}^{(2)}(a)}{\overline{SC}^{5/6}}+\frac{F_{12}^{(2)}(b)}{\sqrt{\overline{SC}}}+\frac{F_{12}^{(2)}(c)}{\overline{SC}^{1/6}}\right),$$

$$G_{12}^{(1)}(3)=-\frac{4^2a_1\alpha_0^2a_r^6C_{44}C_{11}g_1Term(1)Term(3)}{\pi\Delta^*}$$

$$\times\int_{-\pi/2}^{\pi/2}\frac{d\psi\sin2\psi}{g_2^{3/2}(\psi)\sqrt{\tilde{\varpi}}\sqrt{1-\tilde{\varpi}}\left(1+\sqrt{\tilde{\varpi}}\right)}\left(\frac{F_{12}^{(3)}(a)}{\overline{SC}^{5/6}}+\frac{C_{44}}{\overline{SC}^{1/6}}\right);$$

$$G_{13}^{(1)}(1)=\frac{2^7a_1\alpha_0^2a_r^7C_{44}C_{11}\tan\theta\cos\phi Term(1)^2}{3\pi\sqrt{g_1}\Delta^*}$$

$$\times\int_{-\pi/2}^{\pi/2}d\psi\frac{\cos\psi\cos(\psi-\phi)}{g_2^{5/2}(\psi)\tilde{\varpi}\sqrt{1-\tilde{\varpi}}\left(1+\sqrt{\tilde{\varpi}}\right)^2}\left(\frac{F_{13}^{(1)}(a)}{\sqrt{\overline{SC}}}+2C_{11}\overline{SC}^{1/6}+\frac{4C_{12}\cos^2\psi}{\overline{SC}^{1/6}}\right),$$

$$G_{13}^{(1)}(2)=-\frac{2^5a_1\alpha_0^2a_r^6C_{44}C_{11}\cos\phi Term(1)Term(2)}{\pi\Delta^*}$$

$$\times\int_{-\pi/2}^{\pi/2}\frac{d\psi\sin2\psi}{g_2^{3/2}(\psi)\sqrt{\tilde{\varpi}}\sqrt{1-\tilde{\varpi}}\left(1+\sqrt{\tilde{\varpi}}\right)}\left(\frac{F_{13}^{(2)}(a)}{\overline{SC}^{5/6}}+\frac{2C_{11}}{\overline{SC}^{1/6}}-\frac{C_{12}}{\sqrt{\overline{SC}}}\right),$$

$$G_{13}^{(1)}(3)=0;$$

$$G_{21}^{(2)}(m)=-\frac{\alpha_2\sin\phi}{\alpha_1a_r^2g_1(\phi)}G_{12}^{(1)}(m),\qquad m=1,\ 2\text{ and }3;$$

$$G_{22}^{(2)}(1)=\frac{2^7a_1\alpha_0^2a_r^7C_{11}\sqrt{g_1}\tan\theta Term(1)Term(2)}{\pi\Delta^*}\int_{-\pi/2}^{\pi/2}d\psi$$

$$\times \frac{\sin\psi \cos(\psi-\phi)}{g_2^{5/2}(\psi)\tilde{\omega}\sqrt{1-\tilde{\omega}}\left(1+\sqrt{\tilde{\omega}}\right)^2}\left(2C_{11}\left(C_{44}+C_{12}\right)\overline{SC}^{1/6}+\frac{F_{22}^{(1)}(a)}{\sqrt{\overline{SC}}}+\frac{4C_{12}^2\cos^2\psi}{\overline{SC}^{1/6}}\right)$$

,

$$G_{22}^{(2)}(2)=\frac{2^6 a_1\alpha_0^2 a_r^6 C_{11} g_1 Term(1)Term(2)}{\pi\Delta^*}\int_{-\pi/2}^{\pi/2}\frac{d\psi}{g_2^{3/2}(\psi)\sqrt{\tilde{\omega}}\sqrt{1-\tilde{\omega}}\left(1+\sqrt{\tilde{\omega}}\right)}$$

$$\times\left(\frac{F_{22}^{(2)}(a)}{\overline{SC}^{5/6}}+\frac{C_{11}(C_{44}+C_{12})}{\overline{SC}^{1/6}}-\frac{2C_{12}^2\sin^2\psi\cos^2\psi}{\sqrt{\overline{SC}}}\right),$$

$$G_{22}^{(2)}(3)=0\,;$$

$$G_{23}^{(2)}(1)=-\frac{2^5 a_1\alpha_0^2 a_r^6 C_{44}C_{11}\cos\phi Term(1)Term(2)}{\pi\Delta^*}$$

$$\times\int_{-\pi/2}^{\pi/2}\frac{d\psi\sin 2\psi}{g_2^{3/2}(\psi)\sqrt{\tilde{\omega}}\sqrt{1-\tilde{\omega}}\left(1+\sqrt{\tilde{\omega}}\right)}\left(\frac{F_{23}^{(1)}(a)}{\overline{SC}^{5/6}}+\frac{C_{44}}{\overline{SC}^{1/6}}\right),$$

$$G_{23}^{(2)}(2)=\frac{2^7 3 a_1\alpha_0^2 a_r^7 C_{44}C_{11}\tan\theta\cos\phi Term(2)^2}{\pi\sqrt{g_1}\Delta^*}$$

$$\times\int_{-\pi/2}^{\pi/2}d\psi\,\frac{\cos\psi\cos(\psi-\phi)}{g_2^{5/2}(\psi)\tilde{\omega}\sqrt{1-\tilde{\omega}}\left(1+\sqrt{\tilde{\omega}}\right)^2}\left(\frac{F_{23}^{(2)}(a)}{\overline{SC}^{5/6}}+\frac{F_{23}^{(2)}(c)}{\sqrt{\overline{SC}}}+\frac{F_{23}^{(2)}(b)}{\overline{SC}^{1/6}}\right)$$

,

$$G_{23}^{(2)}(3)=\frac{2^4 3 a_1\alpha_0^2 a_r^6 C_{44}C_{11}\cos\phi Term(2)Term(3)}{\pi\Delta^*}$$

$$\times\int_{-\pi/2}^{\pi/2}\frac{d\psi}{g_2^{3/2}(\psi)\sqrt{\tilde{\omega}}\sqrt{1-\tilde{\omega}}\left(1+\sqrt{\tilde{\omega}}\right)}\left(\frac{F_{23}^{(3)}(a)}{\overline{SC}^{5/6}}+\frac{F_{23}^{(3)}(b)}{\overline{SC}^{1/6}}+\frac{F_{23}^{(3)}(c)}{\sqrt{\overline{SC}}}\right);$$

$$G_{31}^{(3)}(m)=\frac{\alpha_3\tan\phi}{\alpha_1 a_r^2}G_{13}^{(1)}(m),\qquad m=1,\,2\text{ and }3;$$

$$G_{32}^{(3)}(m)=-\frac{\alpha_3 g_1(\phi)}{\alpha_2\cos\phi}G_{23}^{(2)}(m),\qquad m=1,\,2\text{ and }3;$$

$$G_{33}^{(3)}(1)=\frac{2^6 a_1\alpha_0^2 a_r^7 C_{11}^2\tan\theta\cos\phi Term(1)Term(3)}{\pi\sqrt{g_1}\Delta^*}\int_{-\pi/2}^{\pi/2}d\psi$$

$$\times\frac{\sin\psi\cos(\psi-\phi)}{g_2^{5/2}(\psi)\tilde{\omega}\sqrt{1-\tilde{\omega}}\left(1+\sqrt{\tilde{\omega}}\right)^2}\left(2\left(C_{11}+C_{44}\right)\overline{SC}^{1/6}+\frac{F_{33}^{(1)}(a)}{\sqrt{\overline{SC}}}+\frac{4C_{12}\cos^2\psi}{\overline{SC}^{1/6}}\right),$$

$$G_{33}^{(3)}(2) = \frac{2^5 3 a_1 \alpha_0^2 a_r^6 C_{11} \cos\phi Term(2) Term(3)}{\pi \Delta^*}$$
$$\times \int_{-\pi/2}^{\pi/2} \frac{d\psi}{g_2^{3/2}(\psi)\sqrt{\tilde{\omega}}\sqrt{1-\tilde{\omega}}\left(1+\sqrt{\tilde{\omega}}\right)} \left(\frac{F_{33}^{(2)}(a)}{SC^{5/6}} + \frac{F_{33}^{(2)}(b)}{SC^{1/6}} + \frac{F_{33}^{(2)}(c)}{\sqrt{SC}} \right),$$
$$G_{33}^{(3)}(3) = 0;$$
$$\Delta^* = \sqrt{(1-a_r^2)^2 \sin^2 2\phi + 8 a_r^4 g_1^2(\phi)} \quad (33)$$

Associated average $< G >$ value can be defined as

$$< G >= \frac{1}{\pi/2} \int_0^{\pi/2} d\phi G(P_0) = < G > (\sigma_{ij}^A, \theta_0, \phi_0, a_1, \tan\theta, a_r, C_{nm}), \quad (34)$$

being function of various mentioned parameters.

IV - DISCUSSION

The crack extension force $G(P_0)$ (33), per unit length of the crack front, at P_0 invokes an integration with respect to angular variable ψ. In ***k'*** spaces involved in the Fourier forms of the dislocation elastic fields (see (8), (10) and (12)), we have used the relations $k_1' = \eta_1 \sin\psi$ and $k_3' = \eta_1 \cos\psi$. The integrations with respect to η_1 have provided functions like $\mathrm{Re}(Q_1)$ and $\mathrm{Re}(I_2)$ in stress expressions (see *Appendix B*); remain those with respect to ψ. Various factors and terms in $G(P_0)$ contain ψ, so the integrations with respect to ψ appears laborious and rather unnecessary because the physical parameters (σ_{ij}^A, a_1, θ, a_r and C_{nm}) are revealed in $G(P_0)$ (33). The average form $< G >$ (34) of $G(P_0)$ is function of various parameters: cubic elastic constants C_{nm} that measure the elastic anisotropy of the medium; $a_r = a_1 / a_2$, the ratio of the semiaxes a_1 and a_2 along x_1' and x_3', that is a measure of the departure from the isotropic medium where $a_r = 1$ in steady motion [1 - 3]; angle θ, evaluated at the height $h = a_1 \tan\theta$, provides a knowledge of the lateral shape of the conoidal crack during its growing; σ_{ij}^A the applied stress matrix with respect to the laboratory reference frame Ox_j; θ_0 and ϕ_0 (Euler's angles) provide the connexion between Ox_j and $O x_j'$ attached to the conoidal crack. Generally, three Euler's angles are needed. Here ***(Figure 1)*** only two (θ_0 and ϕ_0) are used because x_3 is contained in the plane $O x_1' x_3'$ with normal x_2' . Consider a material that deforms under

loading. The energy E of the system (potential energy of the loading mechanism and the elastic energy of the medium) decreases during its evolution. The material adopts the appropriate possible (depending on external conditions of imposed stress, strain rate and temperature) deformation mode that insures highest energy decrease. The description that follows apply to numerous materials. We refer to copper [6 - 10]. Deformation modes observed are :
(1) Plastic deformation by perfect dislocations observable by transmission electron microscopy (TEM). The microstructure after deformation consists of dislocation walls parallel and perpendicular to active {111} slip planes. When the temperature is sufficiently high, subboundaries are formed that closely satisfy the Frank criterion (subboundary in equilibrium with no long-range stress fields in the medium).
(2) Abundant mechanical twinning which results from the motion of imperfect dislocations. This occurs above 773K at a well-defined applied stress level τ_V (thermally activated) which defines the beginning of stage V deformation. The twinning develops at various points in the sample and occupies volumes of the order of several mm^3. It seems that this twinning results from the nucleation and propagation of a nucleus that grows in a regular manner over large distance; this may be described in a similar manner as for the crack presented in *Section* 1(use ***Figure* 1**). We thus take up the idea of our predecessors ([5, 11], for example) who cover the boundary of the nucleus of a mechanical twin by dislocations (see Fig. 6.35 in [11]). The loaded material develops twins to decrease the energy E of the system in the same way as with cracks. Hence, the present study also entirely applies to twin with the following modification: $(\sigma')^{A}$ is to be replaced by $(\sigma')^{A\text{-}Fr}$ in (14) and $(\sigma)^{A}$ (*Appendix A*) by $(\sigma)^{A\text{-}Fr}$ given by

$$(\sigma)^{A-Fr}=\begin{pmatrix} -\nu_A(1)(\sigma_{22}^{a}-\sigma_{22}^{fr}) & \sigma_{12}^{a}-\sigma_{12}^{fr} & 0 \\ \sigma_{21}^{a}-\sigma_{21}^{fr} & \sigma_{22}^{a}-\sigma_{22}^{fr} & \sigma_{23}^{a}-\sigma_{23}^{fr} \\ 0 & \sigma_{32}^{a}-\sigma_{32}^{fr} & -\nu_A(3)(\sigma_{22}^{a}-\sigma_{22}^{fr}) \end{pmatrix}_{x_j} \quad (35)$$

where σ_{ij}^{fr} is the friction stress opposing the motion of the twin dislocations in the medium. Confrontations with experiments will form *Part II* of this study with attention to the activation of twins in stage V in [112] copper single crystals deformed at constant strain rates in temperature regime 2 [6 - 8]. The following twinning has been identified (see Fig. 87, page 140, in [6]) :

(*i*) $K_1 \equiv (1\bar{1}1) = x_1^{'}x_3^{'}$ twinning plane

(*ii*) $\eta_1 \equiv [121]$ the shear direction $x_1^{'}$

(*iii*) $K_2 \equiv (111)$ second undeformed plane

(iv) $\eta_2 \equiv [\bar{1}2\bar{1}]$ intersection of the plane of shear $(10\bar{1}) = x_1^{'}x_2^{'}$ and plane K_2

In ***Figure 1***, we have

$$\vec{x}_1 = \left[\bar{2}4\bar{1}\right]/\sqrt{21}, \quad \vec{x}_2 = \left[112\right]/\sqrt{6}, \quad \vec{x}_3 = \left[31\bar{2}\right]/\sqrt{14},$$
$$\theta_0 = 62°, \quad \phi_0 = 19°. \tag{36}$$

V - CONCLUSION

The present study considers a conoidal crack of finite dimensions, inside an infinitely extended elastic cubic material, in the form of a continuous distribution of infinitesimal dislocations. The vertex O is taken as the origin of an attached Cartesian system (O; $x_j^{'}$), ***Figure 1***. $O\,x_2^{'}$ is the symmetrical axis and the bases are elliptical in $x_1^{'}x_3^{'}$ planes with semiaxes ρ_1 and ρ_2 (at elevation $x_2^{'} = OO'$) along $x_1^{'}$ and $x_3^{'}$, respectively. $a_r = \rho_1 / \rho_2$ is a measure of the departure from isotropy (a_r =1). A laboratory reference frame (O; x_j) is used to specify uniformly applied stresses at infinity: tension σ_{22}^{a} and shears σ_{21}^{a} and σ_{23}^{a} along x_2, x_1 and x_3 directions, respectively. Under such conditions, the crack contains three dislocation families m (m = 1, 2 and 3) with Burger's vectors $\boldsymbol{b}_m = b\ \vec{x}_m^{'}$. Expressions for the elastic fields (displacement and stress) of the dislocations are provided. Spatial forms about the crack-tip of the crack dislocation distribution D_m, at equilibrium, are obtained with associated relative displacement ϕ_m of the faces of the crack. These lead to analytical expressions for crack-tip stresses and crack extension force G per unit length of the crack front. By using "twin" instead of "crack", it is stressed that this study also applies entirely when macroscopic twinning is the mode of deformation adopted by the loaded cubic material. For definiteness, is exemplified the abundantly observed mechanical twinning in temperature regime 2 (773- 1173K) in [112] copper single crystals, deformed at constant strain rates (stage V).

REFERENCES

[1] - P. N. B. ANONGBA, Rough conoidal crack under general loading : dislocation, crack-tip stress, and crack extension force, *Rev. Ivoir. Sci. Technol.*, 40 (2022) 177 - 206

[2] - P. N. B. ANONGBA, Rough conoidal crack under general loading : crack extension force as a function of the average cone angle, *ResearchGate*, (2022), DOI: 10.13140/RG.2.2.13078.01600

[3] - P. N. B. ANONGBA, Elliptical crack under arbitrarily applied loadings : dislocation, crack-tip stress and crack extension force, *Rev. Ivoir. Sci. Technol.*, 38 (2021) 388 - 409

[4] - T. MURA, The continuum theory of dislocations, In: "Advances in Materials Research" (Edited by H. Herman), Interscience Publications, Vol. 3, (1968) 1 - 108

[5] - B. A. BILBY and J. D. ESHELBY, Dislocations and the theory of fracture, In: "Fracture", Ed. Academic Press (H. Liebowitz), New York, Vol. 1, (1968) 99 - 182

[6] - P. N. B. ANONGBA, Doctorate thesis No. 826, EPFL, Lausanne, (1989)

[7] - P. N. B. ANONGBA, J. BONNEVILLE and J.-L. MARTIN, Hardening stages of [112] copper single crystals at intermediate and high temperature- I. Mechanical behaviour, *Acta metal. Mater.*, 41 (1993) 2897 - 2906

[8] - P. N. B. ANONGBA, J. BONNEVILLE and J.-L. MARTIN, Hardening stages of [112] copper single crystals at intermediate and high temperature- II. Slip systems and microstructures, *Acta metal. Mater.*, 41 (1993) 2907 - 2922

[9] - P. N. B. ANONGBA and J.-L. MARTIN, Dislocation clustering and hardening of copper, Proceedings of the 9th International Conference of the Strength of Materials (ICSMA – 9), Haifa, Israel, Vol. 1, (1991) 203 - 210

[10] - P. N. B. ANONGBA, Subboundary structures in stage IV in [112] copper single crystals deformed at high temperatures, Proceedings of the 7th JIM International Symposium (JIMIS – 7) on Aspects of High Temperature Deformation and Fracture in Crystalline Materials, Nagoya, Japan, (1993) 11 - 18

[11] - J. FRIEDEL, "Dislocations", Pergamon Press, Paris, (1964)

APPENDIX A: APPLIED STRESSES $(\sigma')^A$ (*Section* 2.2)

$$\sigma'^{A}_{11} = \cos^2\phi_0\left(\cos^2\theta_0\sigma^A_{11} + \sin^2\theta_0\sigma^A_{22}\right) + \sin^2\phi_0\sigma^A_{33} + \sin 2\theta_0\cos^2\phi_0\sigma^A_{12} + \sin 2\phi_0\sin\theta_0\sigma^A_{23}$$

$$\sigma'^{A}_{22} = \sin^2\theta_0\sigma^A_{11} - \sin 2\theta_0\sigma^A_{12} + \cos^2\theta_0\sigma^A_{22}$$

$$\sigma'^{A}_{33} = \sin^2\phi_0\cos^2\theta_0\sigma^A_{11} + \sin 2\theta_0\sin^2\phi_0\sigma^A_{12} - \sin 2\phi_0\cos\theta_0\sigma^A_{31} + \sin^2\phi_0\sin^2\theta_0\sigma^A_{22} - \sin 2\phi_0\sin\theta_0\sigma^A_{23} + \cos^2\phi_0\sigma^A_{33}$$

$$\sigma'^{A}_{12} = \sin 2\theta_0\cos\phi_0\left(\sigma^A_{22} - \sigma^A_{11}\right)/2 + \cos\phi_0\cos 2\theta_0\sigma^A_{21} - \sin\phi_0\sin\theta_0\sigma^A_{31} + \sin\phi_0\cos\theta_0\sigma^A_{23}$$

$$\sigma'^{A}_{13} = -\sin 2\phi_0\left(\cos^2\theta_0\sigma^A_{11} + \sin^2\theta_0\sigma^A_{22} - \sigma^A_{33}\right)/2 - \sin 2\phi_0\sin 2\theta_0\sigma^A_{21}/2 + \cos 2\phi_0\left(\cos\theta_0\sigma^A_{31} + \sin\theta_0\sigma^A_{23}\right)$$

$$\sigma'^{A}_{23} = -\sin 2\theta_0\sin\phi_0\left(\sigma^A_{22} - \sigma^A_{11}\right)/2 + \cos\phi_0\cos\theta_0\sigma^A_{23} - \sin\phi_0\cos 2\theta_0\sigma^A_{21} - \sin\theta_0\cos\phi_0\sigma^A_{31};$$

$$(\sigma)^A = \begin{pmatrix} -\nu_A(1)\sigma^a_{22} & \sigma^a_{12} & 0 \\ \sigma^a_{21} & \sigma^a_{22} & \sigma^a_{23} \\ 0 & \sigma^a_{23} & -\nu_A(3)\sigma^a_{22} \end{pmatrix}_{x_j}.$$

$\nu_A(m)$ (m= 1 and 3) is Poisson's ratio in the direction x_m perpendicular to the applied tension x_2.

APPENDIX B: CRACK DISLOCATION (*m*) STRESSES $\sigma^{(m)}_{ij}(\vec{x}';\rho_1)$ (*Section* 3.1)

$$\sigma^{(1)}_{11}(\vec{x}';\rho_1) = \frac{b\rho_1}{2\pi 3C_{11}}\int_{-\pi/2}^{\pi/2} d\psi\,\frac{\sin\psi}{\sqrt{g_2(\psi)}}(x'_2 - h)\,\mathrm{Re}(I_2) \times\left(2\left(C_{12}C_{44} + C^2_{11}\right)\overline{SC}^{1/6} - \frac{F^{(1)}_{11}(a)}{\sqrt{\overline{SC}}} + \frac{4C_{12}C_{11}\cos^2\psi}{\overline{SC}^{1/6}}\right),$$

$$\overline{SC} = \sin^6\psi + \cos^6\psi,\; g_2(\psi) = \cos^2\psi + a_r^2\sin^2\psi,$$

$$F^{(1)}_{11}(a) = \sin^4\psi C_{11}(C_{12} + C_{44}) + \cos^4\psi C_{11}(C_{12} + C_{11}) - 2C^2_{12}\sin^2\psi\cos^2\psi;$$

$$\sigma^{(2)}_{11} = \frac{b\rho_1}{\pi 3C_{11}}\int_{-\pi/2}^{\pi/2}\frac{d\psi}{\sqrt{g_2(\psi)}}\mathrm{Re}(Q_1)\left(\frac{\sin^2\psi F^{(2)}_{11}(a) + C_{12}\cos^2\psi F^{(2)}_{11}(b)}{\overline{SC}^{5/6}}\right.$$

$$+\frac{F_{11}^{(2)}(c)}{\overline{SC}^{1/6}}-\frac{C_{12}(C_{11}+C_{12})\sin^2\psi\cos^2\psi}{\sqrt{\overline{SC}}}\Bigg),$$

$$F_{11}^{(2)}(a)=F_{11}^{(1)}(a),\quad F_{11}^{(2)}(c)=\sin^2\psi(C_{12}C_{44}+C_{11}^2)+\cos^2\psi C_{12}(C_{11}+C_{44})$$

$$F_{11}^{(2)}(b)=2\sin^4\psi C_{11}+\cos^4\psi(C_{11}+C_{44})-2C_{12}\sin^2\psi\cos^2\psi;$$

$$\sigma_{11}^{(3)}(\vec{x}';\rho_1)=0;$$

$$\sigma_{22}^{(1)}(\vec{x}';\rho_1)=\frac{b\rho_1}{2\pi 3C_{11}}\int_{-\pi/2}^{\pi/2}d\psi\,\frac{\sin\psi}{\sqrt{g_2(\psi)}}(x_2'-h)\,\mathrm{Re}(I_2)$$

$$\times\left(2C_{11}\left(C_{44}+C_{12}\right)\overline{SC}^{1/6}+\frac{F_{22}^{(1)}(a)}{\sqrt{\overline{SC}}}+\frac{4C_{12}^2\cos^2\psi}{\overline{SC}^{1/6}}\right),$$

$$F_{22}^{(1)}(a)=-\left(\sin^4\psi(C_{11}^2+C_{12}C_{44})+\cos^4\psi C_{11}(C_{12}+C_{11})-2C_{12}C_{11}\sin^2\psi\cos^2\psi\right)$$

;

$$\sigma_{22}^{(2)}=\frac{b\rho_1}{\pi 3C_{11}}\int_{-\pi/2}^{\pi/2}\frac{d\psi\,\mathrm{Re}(Q_1)}{\sqrt{g_2(\psi)}}\left(\frac{F_{22}^{(2)}(a)}{\overline{SC}^{5/6}}+\frac{C_{11}(C_{44}+C_{12})}{\overline{SC}^{1/6}}-\frac{2C_{12}^2\sin^2\psi\cos^2\psi}{\sqrt{\overline{SC}}}\right),$$

$$F_{22}^{(2)}(a)=C_{11}^2(\sin^4\psi+\cos^4\psi)-C_{11}C_{12}\sin^2\psi\cos^2\psi+C_{12}C_{44}\overline{SC};$$

$$\sigma_{22}^{(3)}(\vec{x}';\rho_1)=0;$$

$$\sigma_{33}^{(1)}(\vec{x}';\rho_1)=\frac{b\rho_1}{6\pi}\int_{-\pi/2}^{\pi/2}d\psi\,\frac{\sin\psi}{\sqrt{g_2(\psi)}}(x_2'-h)\,\mathrm{Re}(I_2)$$

$$\times\left(2\left(C_{11}+C_{44}\right)\overline{SC}^{1/6}+\frac{F_{33}^{(1)}(a)}{\sqrt{\overline{SC}}}+\frac{4C_{12}\cos^2\psi}{\overline{SC}^{1/6}}\right),$$

$$F_{33}^{(1)}(a)=-\left(2\cos^4\psi C_{11}+\sin^4\psi(C_{11}+C_{44})-2C_{12}\sin^2\psi\cos^2\psi\right);$$

$$\sigma_{33}^{(2)}=\frac{b\rho_1}{\pi 3C_{11}}\int_{-\pi/2}^{\pi/2}\frac{d\psi\,\mathrm{Re}(Q_1)}{\sqrt{g_2(\psi)}}\left(\frac{F_{33}^{(2)}(a)}{\overline{SC}^{5/6}}+\frac{F_{33}^{(2)}(b)}{\overline{SC}^{1/6}}+\frac{F_{33}^{(2)}(c)}{\sqrt{\overline{SC}}}\right),$$

$$F_{33}^{(2)}(a)=C_{11}C_{12}(\sin^4\psi+\cos^4\psi)-2C_{12}^2\sin^2\psi\cos^2\psi+C_{12}C_{44}\sin^6\psi$$

$$+C_{11}C_{12}\sin^2\psi\cos^4\psi+C_{11}C_{44}\cos^6\psi+C_{11}^2\sin^4\psi\cos^2\psi,$$

$$F_{33}^{(2)}(b)=C_{44}C_{12}+C_{11}C_{12}\sin^2\psi+C_{11}^2\cos^2\psi,$$

$$F_{33}^{(2)}(c)=-C_{12}(C_{11}+C_{12})\sin^2\psi\cos^2\psi;$$

$$\sigma_{33}^{(3)}(\vec{x}';\rho_1)=0; \qquad (B.1)$$

$$\sigma_{12}^{(1)}=\frac{C_{44}b\rho_1}{C_{11}6\pi}\int_{-\pi/2}^{\pi/2}\frac{d\psi\,\mathrm{Re}(Q_1)}{\sqrt{g_2(\psi)}}\left(\frac{F_{12}^{(1)}(a)}{\overline{SC}^{5/6}}+\frac{F_{12}^{(1)}(c)}{\overline{SC}^{1/6}}+\frac{F_{12}^{(1)}(b)}{\sqrt{\overline{SC}}}\right),$$

$$F_{12}^{(1)}(a)=2\left(C_{11}\sin^2\psi\cos^4\psi-2C_{12}\sin^4\psi\cos^2\psi-C_{11}\cos^6\psi\right),$$
$$F_{12}^{(1)}(b)=C_{44}\sin^4\psi+C_{11}\cos^4\psi,\quad F_{12}^{(1)}(c)=2\left(C_{44}\sin^2\psi-2C_{12}\cos^2\psi\right);$$

$$\sigma_{12}^{(2)}(\vec{x}';\rho_1)=-\frac{C_{44}b\rho_1}{C_{11}6\pi}\int_{-\pi/2}^{\pi/2}d\psi\,\frac{\sin\psi}{\sqrt{g_2(\psi)}}(x_2'-h)\,\mathrm{Re}(I_2)$$
$$\times\left(\frac{F_{12}^{(2)}(a)}{\overline{SC}^{5/6}}+\frac{F_{12}^{(2)}(b)}{\sqrt{\overline{SC}}}+\frac{F_{12}^{(2)}(c)}{\overline{SC}^{1/6}}\right),$$

$$F_{12}^{(2)}(a)=2\left(C_{11}(\sin^4\psi+\cos^4\psi)-2C_{12}\sin^2\psi\cos^2\psi-C_{11}\overline{SC}\right),$$
$$F_{12}^{(2)}(c)=2\left(C_{44}-2C_{12}\cos^2\psi\right),\quad F_{12}^{(2)}(b)=C_{44}\sin^4\psi+C_{11}\cos^4\psi;$$

$$\sigma_{12}^{(3)}=\frac{C_{44}b\rho_1}{C_{11}6\pi}\int_{-\pi/2}^{\pi/2}d\psi\,\frac{\sin 2\psi}{\sqrt{g_2(\psi)}}\mathrm{Re}(Q_1)\left(\frac{F_{12}^{(3)}(a)}{\overline{SC}^{5/6}}+\frac{C_{44}}{\overline{SC}^{1/6}}\right),$$
$$F_{12}^{(3)}(a)=C_{11}(\sin^4\psi+\cos^4\psi)-2C_{12}\sin^2\psi\cos^2\psi;$$

$$\sigma_{13}^{(1)}(\vec{x}';\rho_1)=-\frac{C_{44}b\rho_1}{C_{11}6\pi}\int_{-\pi/2}^{\pi/2}d\psi\,\frac{\cos\psi}{\sqrt{g_2(\psi)}}(x_2'-h)\,\mathrm{Re}(I_2)$$
$$\times\left(\frac{F_{13}^{(1)}(a)}{\sqrt{\overline{SC}}}+2C_{11}\overline{SC}^{1/6}+\frac{4C_{12}\cos^2\psi}{\overline{SC}^{1/6}}\right),$$
$$F_{13}^{(1)}(a)=-\left(C_{44}\sin^4\psi+C_{11}\cos^4\psi\right);$$

$$\sigma_{13}^{(2)}=\frac{C_{44}b\rho_1}{C_{11}6\pi}\int_{-\pi/2}^{\pi/2}d\psi\,\frac{\sin 2\psi}{\sqrt{g_2(\psi)}}\mathrm{Re}(Q_1)\left(\frac{F_{13}^{(2)}(a)}{\overline{SC}^{5/6}}+\frac{2C_{11}}{\overline{SC}^{1/6}}-\frac{C_{12}}{\sqrt{\overline{SC}}}\right),$$

$$F_{13}^{(2)}(a)=(C_{11}+C_{44})(\sin^4\psi+\cos^4\psi);$$
$$\sigma_{13}^{(3)}(\vec{x}';\rho_1)=0;$$

$$\sigma_{23}^{(1)}=\frac{C_{44}b\rho_1}{C_{11}6\pi}\int_{-\pi/2}^{\pi/2}d\psi\,\frac{\sin 2\psi}{\sqrt{g_2(\psi)}}\mathrm{Re}(Q_1)\left(\frac{F_{23}^{(1)}(a)}{\overline{SC}^{5/6}}+\frac{C_{44}}{\overline{SC}^{1/6}}\right),$$
$$F_{23}^{(1)}(a)=C_{11}(\sin^4\psi+\cos^4\psi)-2C_{12}\sin^2\psi\cos^2\psi;$$

$$\sigma_{23}^{(2)}(\vec{x}';\rho_1)=-\frac{C_{44}b\rho_1}{C_{11}6\pi}\int_{-\pi/2}^{\pi/2}d\psi\,\frac{\cos\psi}{\sqrt{g_2(\psi)}}(x_2'-h)\,\mathrm{Re}(I_2)$$
$$\times\left(\frac{F_{23}^{(2)}(a)}{\overline{SC}^{5/6}}+\frac{F_{23}^{(2)}(c)}{\sqrt{\overline{SC}}}+\frac{F_{23}^{(2)}(b)}{\overline{SC}^{1/6}}\right),$$

$$F_{23}^{(2)}(a) = F_{12}^{(2)}(a), \quad F_{23}^{(2)}(b) = 2\left(C_{44} - 2C_{12}\sin^2\psi\right),$$
$$F_{23}^{(2)}(c) = C_{11}\sin^4\psi + C_{44}\cos^4\psi;$$

$$\sigma_{23}^{(3)} = \frac{C_{44} b \rho_1}{C_{11} 6\pi} \int_{-\pi/2}^{\pi/2} d\psi \, \frac{\mathrm{Re}(Q_1)}{\sqrt{g_2(\psi)}} \left(\frac{F_{23}^{(3)}(a)}{\overline{SC}^{5/6}} + \frac{F_{23}^{(3)}(b)}{\overline{SC}^{1/6}} + \frac{F_{23}^{(3)}(c)}{\sqrt{\overline{SC}}} \right),$$
$$F_{23}^{(3)}(a) = 2\left(C_{11}\cos^2\psi(\sin^4\psi + \cos^4\psi) - 2C_{12}\sin^2\psi\cos^4\psi - C_{11}\overline{SC}\right),$$
$$F_{23}^{(3)}(b) = 2\left(C_{44}\cos^2\psi - 2C_{12}\sin^2\psi\right), \quad F_{23}^{(3)}(c) = F_{23}^{(2)}(c); \qquad (B.2)$$

$$\mathrm{Re}(Q_1) = \frac{\bar{y}_1}{\left(\bar{y}_1^2 - \Omega^2\right)^{3/2}} \text{ and } \quad \mathrm{Re}(I_2) = -\frac{3\bar{y}_1\Omega}{\left(\bar{y}_1^2 - \Omega^2\right)^{5/2}}, \qquad \Omega < \bar{y}_1 \text{ for both,}$$

where $\bar{y}_1 = \dfrac{\rho_1}{a_r}\sqrt{g_2(\psi)}$, $g_2(\psi) = \cos^2\psi + a_r^2\sin^2\psi$ and $\Omega = \sin\psi x_1' + \cos\psi x_3'$